Properties and geoeffectiveness of halo CMEs

G. Michalek

Astronomical Observatory of Jagiellonian University, Cracow, Poland

N. Gopalswamy

NASA Goddard Space Flight Center, Greenbelt, MD 20771, USA

A. Lara

Instituto de Geofísica, UNAM, México

S. Yashiro

Center for Solar and Space Weather, Catholic University of America

Abstract. Halo coronal mass ejections (HCMEs) originating from regions close to the center of the Sun are likely to be geoeffective. Assuming that the shape of HCMEs is a cone and they propagate with constant angular widths and velocities, at least in their early phase, we have developed a technique (Michalek et al. 2003) which allowed us to obtain the space speed, width and source location. We apply this technique to obtain the parameters of all full HCMEs observed by the Solar and Heliospheric Observatory (SOHO) mission's Large Angle and Spectrometric Coronagraph (LASCO) experiment until the end of 2002. Using this data we examine which parameters determine the geoeffectiveness of HCMEs. We show that in the considered period of time only fast halo CMEs (with the space velocities higher than $\sim 1000\frac{km}{s}$ and originating from the western hemisphere close to the solar center could cause the severe geomagnetic storms. We illustrate how the HCME parameters can be used for space weather forecast. It is also demonstrated that the strength of a geomagnetic storm does not depend on the determined width of HCMEs. This means that HCMEs do not have to be very large to cause major geomagnetic storms.

1. Introduction

Coronal mass ejections (CMEs) originating from regions close to the central meridian of the Sun and directed toward Earth cause the most severe geomagnetic storms (Gosling, 1993; Kahler, 1992; Webb et al., 2001). Many of these Earth-directed CMEs appear as an enhancement surrounding the occulting disk of coronagraphs. We call them halo CMEs (Howard et al. 1982). The measured properties of CMEs include their occurrence rate, direction of propagation in the plane of the sky, angular width, and speed (e.g. Kahler, 1992; Webb, 2000; St. Cyr et al., 2000, Gopalswamy et al., 2003a; Gopalswamy, 2004; Yashiro et al., 2004). It is well known that the geoffective CMEs originate mostly within a latitude $\pm 30^o$ (Gopalswamy et al., 2000a, 2001; Webb et al., 2000, 2001; Wang et al., 2002; Zhang et al. 2003). Srivastava and Venkatakrishan (2002) showed that the initial speed of the CMEs is correlated with the D_{ST} index strength of the geomagnetic storm, although their conclusion was based only on the study of four events. This tendency was also suggested earlier by Gosling et al. (1990) and Tsurutani & Gonzalez (1998). On the other hand, Zhang et al. (2003) demonstrated that both slow and fast HCMEs can cause major geomagnetic disturbances. They showed that geoeffective CMEs are more likely to originate from the western hemisphere than from the eastern hemisphere. They also demonstrated a lack of correlation between the size of X-ray associated with a given CME and the importance of geomagnetic storms. Unfortunately, these studies were based on the sky plane speeds of CMEs without consideration of the projection effects. The parameters describing properties of CMEs, especially for HCMEs, are affected by projection effects (Gopalswamy et al., 2000b). Assuming that the shape of HCMEs is a cone and they propagate with constant angular widths and speeds, at least in their early phase of propagation, we have developed a technique (Michalek et al. 2003) which allows us to determine the following parameters: the linear distance r of source location measured from the solar disk center, the angular distance γ of source location measured from the plane of sky, the angular width α (cone angle $=0.5\alpha$) and the space velocity V of a given HCME. A similar cone model was used recently by Xie et al. (2004) to determine the angular width and orientation of HCMEs.

The present paper is divided into two parts. First, in the Section 2 we applied the cone model (Michalek et al. 2003) to obtain the space parameters of all HCMEs observed by the Solar and Heliospheric Observatory (SOHO) mission's Large Angle and Spectrometric Coronagraph (LASCO) until the end of 2002. In the Subsection 2.2 a short statistical analysis, based on the derived parameters, of HCMEs is presented (Fig. 1 - Fig. 4). In the Section 3, we use these parameters to identify the most important factors determining geoeffectiveness of HCMEs and how they could be used for space weather forecast (Fig. 5 - Fig. 17)

2. Space parameters of HCMEs

2.1. Data

The list of HCMEs studied in this paper is shown in Table 1. We considered only frontside full (type F) and asymmetric (type A) HCMEs (Gopalswamy et al. 2003b). Only these events could be considered using the technique proposed by Michalek et al. (2003). Full halos are the classical halo CMEs which originate from close the disk center. Asymmetric halos are typically wide, near-limb CMEs, which become halos late in the event. They are different from partial halos. The partial halos never appear around

the entire oculting disk, even in LASOC/C3 observations (their width is $< 360^o$). Only frontside events could be potentially geoeffective. The first four columns of Table 1 are from the SOHO/LASCO catalog (date, time of first appearance in the coronagraph field of view, projected speed and position angle of the fastest part of the HCME). Details about the SOHO/LASCO catalog and the method of measurements are described by Yashiro et al. (2004). Parameters r, γ, α, and V, estimated from the cone model (Michalek et al. 2003), are shown in columns (5), (6), (7), and (8), respectively. It is important to note that for some events, the space velocity determined by this technique could be smaller than the projected speeds reported in the LASCO catalog. This is because the Michalek et al. (2003) technique applies only to the beginning phase of CMEs, whereas the CME catalog gives average speed within the LASCO's field of view. The model also cannot estimate the parameters for symmetric HCMEs originating very close to the disk center and for limb events appearing as halos on account of deflections of preexisting coronal structures. In column (9) the source locations of the associated H-flares are given. The associated flares were determined using two restrictions. They should originate in the same part of solar disk and set up in the same time as respective CMEs (limit time is about half an hour). To be sure that our determination is correct we checked together EIT and LASCO movies also. It is important to note that localization of solar flares might be slightly shifted with respect to origin of CMEs. This might affect some figures and presented correlations. By examining the solar wind plasma data from Solar Wind Experiment (Wind/SWE, http://web.mit.edu/space/www/wind/) and interplanetary magnetic field data (from Magnetic Field Investigation, http://lepmfi.gsfc.nasa.gov/mfi), we identified, when possible, the associated interplanetary CMEs (ICMEs). The changes of geomagnetic indices D_{ST} and Ap caused by these ICMEs are presented in columns 10 and 11, respectively. The last two columns give the maximum value of magnitude (B) and southward component (B_Z) of magnetic field in the ICME. We considered 144 frontside HCMEs (FHCMEs) recorded by the LASCO coronagraphs until the end of 2002. For 101(70%) of them we were able to determine the required parameters (r, γ, α, and V). The events that could not be measured were mostly too faint to get height-time plots at the opposite sides of the occulting disk. Only a few (16) were symmetric for which we could not obtain the HCME parameters.

2.2. Statistical analysis

2.2.1. The space velocities of FHCMEs

The properties of halo CMEs observed by SOHO/LASCO have been described in a number of papers (Gopalswamy et al., 2003a; Gopalswamy, 2004; Yashiro et al., 2004). Here we describe the properties of FHCMEs measured according to Michalek et al. (2003). Fig. 1 shows the distribution of the space velocities (V) of FHCMEs during the ascending (1996-1999) and maximum phases of solar activity (2000-2002) as well as for the whole period (1996-2002). It was noted before, e.g., by Webb et al. (1999), Gopalswamy (2004, see Fig 1.13, 1.14) and Yashiro et al. (2004), that HCMEs are much faster and more energetic than typical CMEs. Our results also confirm this. The average speed of the HCMEs is $1300 km/s$ (about 25% larger than that for HCMEs from SOHO/LASCO catalog, Yashiro et al. (2004)). The difference, between average speeds received in the present paper and by Yashiro et al. (2004), is likely to be due to the fact that we are using corrected speeds while Yashiro et al. (2004) used sky-plane speeds. We use a smaller number of events in the statistic. From the histograms in Figure 1, it is evident that velocities of HCMEs increase significantly following the solar activity cycle as for all CMEs (Yashiro et al., 2004). During the maximum of solar activity the FHCMEs have, on the average, velocities about 40% higher than the average velocities during the minimum of solar activity. The speed of the slowest event is $189 km/s$ while the speed of the fastest one is $2655 km/s$.

In Fig. 2, we present the sky-plane speeds against the corrected (space) speeds. The solid line represents the linear fit to the data points. The inclination of the linear fit demonstrates that the projection effect increases slightly with the speed of CMEs. It is clear that the projection effect is important, and on average the corrected speeds are 25% higher than the velocities measured in the plane of sky. This was also anticipated based on other considerations (Gopalswamy et al., 2001). It is important to note that both sky-plane and corrected speeds are determined at the same distance ($2R_\odot$) from the disk center.

2.2.2. Widths of FHCMEs

Fig. 3 shows the distribution of the estimated widths (α) of FHCMEs during the ascending (1996-1999) and maximum phases of solar activity (2000-2002) as well as for the whole period (1996-2002). The average width of HCMEs is 120^o (more than twice the average value obtained from the SOHO/LASCO catalog, Yashiro et al., 2004). The average width of HCMEs does not change significantly with solar activity, except for a small increase during the maximum of solar activity. The most narrow HCME has a width of 39^o and the widest one has α as large as 168^o.

2.2.3. Source locations of FHCMEs

Fig. 4 presents the distribution of source location (γ) of FHCMEs during the ascending (1996-1999) and maximum phases of solar activity (2000-2002) and for the whole period (1996-2002). FHCMEs with γ close to 0^o originate near to the solar limb while events with γ close to 90^o originate from the disk center region. Fig. 4 shows that the FHCMEs originate close to the Sun center with a maximum of distribution around $\gamma = 62^o$. The distribution of source location does not depend on the period of solar activity. We have to note that these distributions are slightly biased due to the fact that we neglected 16 symmetric FHCMEs (these CMEs cannot be measured using the cone model). They originate very close to the disk center and should slightly increase the average value of γ.

3. Geoeffectiveness of FHCMEs.

Having defined the parameters describing FHCMEs, we now explore which of theses parameters determine the strength of geomagnetic disturbances. In situ counterparts of frontside HCMEs can be recognized in the magnetic field and plasma measurements as ejecta (EJs) or magnetic clouds (MCs). Magnetic clouds can be identified by the following characteristic properties: (1) the magnetic field strength is higher than the average; (2) the proton temperature is lower than the average; (3) and the magnetic field direction rotates smoothly (Burlaga 1988, 2002, 2003a,b; Lepping et al., 1990). In the present paper we refer to both MCs and EJs as interplanetary CMEs (ICMEs). The presence of these signatures changes from one ICME to an other. By examining the solar wind plasma data we identified, when possible, ICMEs. These ICMEs could be responsible for geomagnetic disturbances. The strength of geomagnetic storms is described by two indices Ap (which measures the general level of geomagnetic activity over the globe) and D_{ST} (which is obtained using magnetometer data from stations near the equator). The maximum values of D_{ST} and Ap indices associated with the ICMEs are presented in Table 1. We included those events for which the D_{ST} index decreased below -25nT. We now examine the relation between the geomagnetic indices and V, α and γ. First in the Subsection 3.1, we consider influence of different parameters on

geoeffectiveness of FHCMEs (Fig. 5 - Fig. 14). In the Subsection 3.2 we try to find which FHCMEs could cause false alarms (Fig. 15 - Fig. 17).

3.1. Geoeffectiveness of FHCMEs

3.1.1. Geoeffectiveness and space velocity (V) of FHCMEs.

Fig. 5 shows the scatter plots of plane of sky speeds versus D_{ST} and Ap indices. Diamond symbols represent events originating from the western hemisphere and cross symbols represent events originating from the eastern hemisphere. The solid lines are the linear fits to the data points associated with eastern events, and the dashed lines are linear fits to data points associated with western events. The dot-dashed vertical lines indicate velocity limits above which HCMEs can cause geomagnetic storms with $D_{ST} \leq -150nT$. These lines were inferred from two events on 1 May 1998 and 2 May 1998. Upon inspection of this figure, it is clear that the major geomagnetic storms can be generated by slow (speeds $\approx 500km/s$) and fast HCMEs originating in the western hemisphere. There is not a significant correlation (correlation coefficients are < 0.50) between the projected speed and geomagnetic indices. Linear and Spearman correlation coefficients are approximately equal 0.35(0.31) for the western and 0.10(0.05) for eastern events, similar to the results of Zhang et al. (2003). The situation is different when we consider the space velocities of HCMEs. In Fig. 6, the scatter plots of V versus D_{ST} and Ap indices are presented. The space velocities are larger than the plane of sky speeds and all events in the panels are shifted to the higher velocity range, especially for the two events on 1 May 1998 and 2 May 1998, which seem to be narrow (width $\approx 40^o$) and three times faster than they appear in LASCO observations (Table 1). Determination of the space velocity is consistent with observations of ICMEs associated with these events. Since, these CMEs needed only ≈ 46 hours to reach Earth (Manoharan et al., 2004, Michalek et al., 2004), they must be very fast. In LASCO observations these CMEs appear faint, suggesting that they seem to be narrow and they could be observed as halos when they are far from the Sun. Upon inspection of this figure, it is clear that only very fast events ($V \geq 1100km/s$) originating in the western hemisphere can cause the biggest geomagnetic storms ($D_{ST} \leq -150nT$). The dot-dashed verticals lines indicate velocity limits above which HCMEs can cause severe geomagnetic storms. We find significant correlation (correlation coefficients are > 0.50) between velocity and geomagnetic indices for the western events. The linear and Spearman correlation coefficients are 0.60(0.54) and 0.62(0.56) for Ap and D_{ST} indices respectively. In contrast there is very little correlation between the space velocity and geomagnetic indices for the eastern events. the linear and spearman correlation coefficients are 0.16(0.04) and 0.07(0.02) for Ap and D_{ST} indices, respectively. Events originating in the eastern hemisphere are not likely to cause major geomagnetic storms. Fig. 7 shows the distribution of the space velocities (V) of FHCMEs, which cause geomagnetic disturbance with D_{ST} index lower than $-25nT$, $-60nT$ and $-100nT$, respectively. These histograms demonstrate again that geoeffectivenes of HCMEs depend on their space velocities and sever geomagnetic storms with $D_{ST} < -100nT$ can be caused by fast CMEs (with $V > 700km/s$) only. The results seem to be different from these reported by Zhang et al. (2003) for the plane of sky speeds. This demonstrates that conclusions based on coronagraphic observations subjected to the projection effects could be incorrect.

3.1.2. Geoeffectiveness and γ of HCMEs.

In Fig. 8 we show the scatter plots of γ versus D_{ST} and Ap indices. Diamond symbols represent events originating from the western hemisphere and cross symbols represent events originating from the eastern hemisphere. The solid lines are the linear fits to the data points associated with eastern events and the dashed lines are linear fits to data points associated with western events. For the eastern events the correlation between γ and geomagnetic indices is not significant. For these events, the linear and Spearman correlation coefficients for Ap and D_{ST} indices are 0.14(0.18) and 0.20(0.38), respectively. In contrast the western events originating close to the disk center ($\gamma \geq 65^o$) are more likely to cause the biggest geomagnetic storms. For these events correlation coefficients for Ap and D_{ST} indices are 0.39(0.38) and 0.35(0.42), respectively. Similar conclusions are obtained when we consider H-alpha flare locations. In Fig. 9 we show the scatter plots of absolute values of longitudes of H-alpha flares associated with HCMEs versus D_{ST} and Ap indices. Diamond symbols represent events originating from the western hemisphere and cross symbols represent events originating from the eastern hemisphere. These results confirm previous conclusion that the western events originating close to the disk center are more likely to cause the biggest geomagnetic storms. We have to note that there is one event on 04 April 2000 which originate far from the disk center (N26W66) and cause the severe geomagnetic storm with $D_{ST} = -288nT$. Now the correlation between longitude and geomagnetic indices is very poor for the western and eastern events as well. The results are proved by histograms presented in Fig. 10. This figure presents the distribution of the longitude of FHCMs which cause geomagnetic disturbance with D_{ST} index lower than $-25nT$, $-60nT$ and $-100nT$. Upon inspection of the histograms, it is clear that the goeffectiveness of CMEs depends on the longitude of source location and that the severe geomagnetic disturbance ($D_{ST} < -100nT$) are mostly caused by the western events originating close to the disk center. During the study period of time there were only two severe geomagnetic storms ($D_{ST} < -100nT$) caused by western events originating far from the disk center. It is important to note that the peak of the longitude distribution is shifted to the west from the disk center.

3.1.3. Geoeffectiveness and angular widths (α) of CMEs

In Fig. 11, we have shown the scatter plots of α against D_{ST} and Ap indices. Cross and diamonds symbols are associated with the eastern and western events, respectively. The solid lines are the linear fits to the data points associated with eastern events and the dashed lines are linear fits to data points associated with western events. Upon inspection of the figures it is clear that the geoeffectiveness of CMEs depends very little on their widths. All considered correlation coefficients are ≤ 0.22. Even severe geomagnetic storms can be caused by both narrow and wide HCMEs. This means that HCMEs do not have to be very large to cause major geomagnetic storms.

3.1.4. Geoeffectivness against velocities and source localization of the FHCMEs

As we demonstrated in the previous subsection, geoeffectiveness of FHCMEs strongly depends on their space velocity V and source location γ. These parameters may be helpful for space weather forecast. In Figs. 12 and 13, Ap and D_{ST} indices versus γ and V are shown in contour plots using the Kriging (Isaacs and Srivastava, 1989) procedure for generating regular grids. The darker the shade, the higher are the Ap and D_{ST} indices. Knowing the source location and space velocity of a given HCME, we can, in a simple way, predict its geoeffectiveness. From the inspection of the picture we see that the strongest geomagnetic storms can occur for fast events originating close to the disk center.

3.1.5. Geoeffectiveness and interplanetary magnetic field (IMF) carried by FHCMEs

Fig. 14 shows the scatter plots of the maximum values of magnitude (B) and southward component (B_Z) of ICME magnetic field versus D_{ST} and A_p indices. The solid lines are linear fits to the data points. This figure clearly confirms that the major geomagnetic storms are generated by CMEs carrying strong magnetic filed with significant southward component. Correlation between these parameters and geomagnetic indices is very large and linear coefficients are approximately equal 0.70 for (B) and (B_Z) as well. Spearman correlation coefficients in this case are slightly smaller and are approximately equal 0.60 for (B) and (B_Z). Spearman correlation coefficients in this case are slightly smaller and are approximately equal 0.60 for (B) and (B_Z). It is due to the fact that they are derived from the rank of variable within the distribution and they are not sensitive to the 4 outlying points with $|B| > 30nT$. Unfortunately, B and B_Z are measured in situ and hence may not be useful for space weather forecast.

3.2. False alarms

Previous studies (e.g. Cane et al., 2000; St. Cyr et al., 2000; Wang et al. 2002) have shown that a large fraction of frontside HCMEs is non-geoeffective. St. Cyr et al. (2000) found that only 20/40 (50%) of all frontside HCMEs during 1996-1998 from SOHO/LASCO caused geomagnetic storms with $K_P \geq 5$. Wang et al. (2002) used a larger data base (March 1997 to December 2000) showed that 59/132 (45%) of frontside HCMEs could result in moderate to severe geomagnetic storms ($K_P \geq 5$) and that the majority of these events occurred within latitude $\pm(10^o - 30^o)$. They also found an asymmetry in the central meridian distance distribution. In the western hemisphere, a geoeffective event could be expected even at $\sim 70^o$. On the eastern side, there were no geoeffective HCMEs outside of 40^o. We performed a similar analysis for our sample of FHCMEs. During the study period, there were only 88/144 FHCMEs with geomagnetic signatures ($D_{ST} > -25nT$) at Earth which means that only 60% of FHCMEs are geoeffective. For 65/88 (73%) of them we determined the space parameters (r, γ, α, and V). If we take into account only those FHCMEs which caused moderate to severe geomagnetic storms ($D_{ST} > -60nT$) the fraction of geoeffective events decreased to 51/144 (36%). It is important to recognize them because they generate "false alarms". In our sample, there were 56/144 (39%) not geoeffective HCMEs. For 36/56 (62%) of them we were able to determine the space parameters (r, γ, α, and V). We now explore why these FHCMEs did not cause geomagnetic disturbances. Fig. 15 presents the distributions of longitude and the space velocities of the 36 non-geoeffective FHCMEs. The histograms show that these events originate from the whole solar disk and have velocities from $100km/s$ up to $2500km/s$. The distributions do not demonstrate any specific signatures characterizing these events. Fig. 16 shows, in the successive panels, the distributions of: the space velocities for FHCMEs originating close to the disk center ($|longitude| < 30^o$), the space velocities for FHCMEs originating close to the limb ($|longitude| > 30^o$), the longitude for slow FHCMEs ($V < 1200km/s$) and the longitude for fast FHCME ($V > 1200km/s$). Upon the inspection of the histograms (the first and last panel in the figure) it is clear that all fast HCMEs ($V > 1200km/s$) originating close to the disk center ($|longitud| < 30^0$) must be geoeffective. There is no false alarm for such events. Slower FHCMEs ($V < 1200km/s$) originating close to the disk center do not have to be geoeffective. In the third panel we note 20 events originating from the disk center but not influencing Earth. On the other hand, even very fast FHCMEs ($V > 1200km/s$) were not geoeffetive when they originated close to the limb. In the fourth panel we have 16 fast FHCMEs originating close to the limb without geomagnetic signatures at Earth. Fig. 17 shows the scatter plot of the space velocities versus longitude for all FHCMEs. Diamond symbols represent goeeffective and cross symbols non-geoeffective FHCMEs. The solid lines are linear fits for non-geoeffective events originating from the east and west hemisphere. For non-geoeffective eastern and western events the linear and Spearman correlation coefficients are very large and equal 0.88(0.87) and 0.79(0.74), respectively. Upon inspection of the figure, it is clear that geoeffective events are faster than the non-geoeffective events originating at the same longitude. It is also clear from the strong correlation that events originating farther form the disk center are faster than those originating close to the disk center. Linear fits to the non-geoeffective events could be considered as lower limits for the space velocities above which a given CME originating at a given longitude could be observed as a halo event. In the vicinity of these fits we see both geoeffective and non-geoeffective FHCMEs. Slightly above these fits we see only geoeffective FHCMEs. It is important to note that the inclination of linear fit to the eastern events is steeper than that for the western events. Eastern events must be faster to appear as halo events or to be geoeffective than western events originating at the same angular distance from the disk center.

Generally our results are consistent with those of previous studies. We would like to emphasize that the geoeffectiveness of HCMEs depends not only on source locations, but also on their space velocity. Having both the parameters improves our ability to forecast whether a given HCME will be geoeffective or not. Non geoeffective events are slow or fast but originating far from disk center. They do not affect magnetosphere. If they are directly ejected to Earth they are slow and disturbed before reach Earth. If they are fast, they are ejected not directly to Earth (events with large longitude) and they only touch magnetosphere by flanks. Unfortunately there is very difficult to give sharp boundary limits dividing CMEs on geoeffective and non geoeffective events. These limits depend not only on CMEs properties but also on condition of interplanetary medium. Approximate limits can be obtain from Fig. 17. Of course, we appreciate that additional parameters such as the strength and orientation of the resulting interplanetary CME are also expected to play a role in deciding the geoeffectiveness. It is difficult to give sharp boundary conditions for non geoeffective events.

4. Summary

In this study we considered the geoeffectiveness of all full HCMEs observed by SOHO/LASCO coronagraphs from the launch in 1995 until the end of 2002. For 101/144 (70%) of full HCMEs we were able to find the source location, width and space velocity using the cone model (Michalek et al., 2003). We must be aware that the cone model is only rough simplification of real events. We know that not all CMEs are perfectly symmetric (Moran and Davila, 2004; Jackson et al., 2004). Most of CMEs could be approximate using cone model but probably for some of them this assumption is unrealistic. Fortunately technique presented by Michalek et al. does not demand perfect symmetry for CMEs. This approach requires measurements of sky-plane speeds and the moments of the first appearance of the halo CMEs above limb at only two opposite points. We are able to determine, with good accuracy, the space velocity and with of a given CME at least in the plane symmetry crossing CMEs at these points. When a given CME could be approximated by the cone model these derived parameters are valid for the entire CME. HCMEs originating very close to the disk center (mostly within a latitude of $\pm 40^o$), are very wide (the

average angular width = 120^o) and are very fast (the average space speed = $1291 km/s$). We find significant (40%) increase in the average space velocities of HCMEs during the maximum of solar activity. These results could suggest that the HCMEs represent a special class of CMEs which are very wide and fast. It is important to note that this "class" of CMEs is defined due to artificial effect caused by coronagraphic observations. Events originating close to the disk center (from SOHO/LASCO point of view) must be wide and fast to appear as HCMEs in LASCO observations. This is not due to localization on the solar disk but due to oculting disk which not only blocks bright photospheric light but also eliminates some narrow and slow events. We have to emphasize that this effect mostly depends on the dimension of oculting disk but in less degree on the sensitivity of instrument. More sensitive instrument can record some poorer events (halos and also not halos so statistic will be similar) but could not register these events which never appear behind occulting disk. Potentially more sensitive instrument could register less energetic events (narrower and slower) and the average velocities and widths (for halos and whole population of CMEs) could be slightly lower but the main relation between the halos and whole population of events will be the same. Fortunately, poor events do not cause a big concern because they are not geoeffective. We do not expect, in the near future, any special programs devoted to looking for less energetic CMEs. Next scientific mission (STEREO) will be mostly dedicated to recognize 3D structure of CMEs. Such fast and wide CMEs are known to be associated with electron and proton acceleration by driving fast mode MHD shocks (e.g., Cane et al., 1987; Gopalswamy et al., 2002a). Using observations from Wind spacecraft, interplanetary magnetic clouds (MC) and geomagnetic disturbances associated to HCMEs were identified. The strength of geomagnetic storms, described by D_{ST} and Ap indices, is highly correlated with the source location and space velocity of a given event. Only HCMEs originating in the western hemisphere, close to the solar center and very fast (space velocity $\geq 1100 km/s$) are likely to cause major geomagnetic storms ($D_ST < -150nT$). Slow HCMEs (space velocity $\leq 1100 km/s$), even originating close to the solar center, may not cause severe geomagnetic disturbances. We have to note that there was one event (04 April 2000), which originated far from disk center and produced a severe geomagnetic storm ($D_{ST} = -288nT$). Probably this storm was not due to an ICME. It was caused by the sheath region ahead of the CME as was reported by Gopalswamy (2002b). We illustrated, using contour maps, how the derived HCME parameters can be useful for space weather forecast. We have to note that geoeffectiveness of events does not depend on their widths.

During our study period we recognized 56/144 (30%) FHCMEs without any geomagnetic signature at Earth. This is significant population of FHCMEs. To distinguish them from the geoeffective events we considered the source locations and space velocities of HCMEs. When both the parameters are available, it becomes easier to assess the geoeffectiveness of HCMEs. We may say that fast FHCMs ($V > 1200 km/s$) originating close to the disk center ($|longitude| < 30^o$) must be geoeffective. For such events there were no false alarms. But, even very fast events originating far from the disk center can be non-geoeffective.

Acknowledgments. This work was done when GM visited the Center for Solar Physics and Space Weather, The Catholic University of America in Washington.
Work done by Grzegorz Michalek was partly supported by *Komitet Badań Naukowych* through the grant PB 0357/P04/2003/25.
Part of this research was also supported by NASA/LWS and NSF/SHINE programs.

References

Burlaga, L.F., et al., 1988, J. Geophys. Res., 93,7217
Burlaga, L.F., et al., 2003a, ApJ, 585, 115893
Burlaga, L.F., et al., 2003b, J. Geophys. Res., 108, SSH2-1
Cane, H.V., et al., 1987, J. Geophys. Res., 92, 9869
Cane, H.V., Richardson, I.G., St.Cyr, O.C.,2000, Geophys. Res. Lett., 27, 3591
Gopalswamy, N., et al. 2000a, Geophys. Res. Lett., 27, 145
Gopalswamy, N., et al. 2000b, Geophys. Res. Lett., 27, 1427
Gopalswamy, N., et al., 2001,J. Geophys. Res., 106, 29207
Gopalswamy, N., et al., 2002a, ApJL, 572, L103
Gopalswamy, N., 2002b, In solar-terrestial magnetic activity ans space environment, Ed. H.N. Wang and R.L. Lin, COSPRA Colloquia Ser., Vol. 14, p157
Gopalswamy, N., et al., 2003a, ApJ, 598,L63
Gopalswamy, N., et al., 2003b, Proc. ISCS 2003 Synposium, Tatranska Lomnica, Slovakia, p403
Gopalswamy, N., 2004, ASSL series, ed. G. Poletto and S. Suess, KLUWER, in press
Gosling J.T., 1993, J. Geophys. Res. , 98, 18937
Gosling J.T., et al., 1990, Geophys. Res. Lett., 17, 901
Howard R.A., et al., 1982, ApJ, 263, L101
Isaacs, E., Srivastava, 1989, An Introduction to Applied Geostatistics.- Oxford University Press, New York.
Jackson, B., et al., 2004, AGU, Fall Meeting 2004, abstract SH21A-0393
Kahler S.W., 1992,Annu. Rev. Astron. Astrophys.,30,113
Lepping, R.P., et al., 1990, J.Geophys.Res., 95, 11957
Manoharan, P.K., et al., 2004 J. Geophys. Res., 109, A06109
Michalek, G., et al., 2003, ApJ, 584, 472
Michalek, G., et al., 2004, A&A, 423,729
Moran, T., Devila, 2004, Science, 305, 66
Srivastava, N., Venkatakrishnan, P., Geophys. Res. Lett., 29, 101029
Sheeley, N.R., Jr., Walters, J.H., Wang, Y.-M., Howard, R.A. 1999, J. Geophys. Res., 104, 24739
St. Cyr, O.C., et al., 2000, J. Geophys. Res., 105, 18169
Tsurutani B.T., Gonzalez W.D., 1998, Geophys. Monogr. 98; Washington, DC,AGU,77
Wang, Y.M., et al., 2002, J. Geophys. Res., 107, 1340
Webb, D.F., et al. 1997, J. Geophys. Res., 102, 24161
Webb, D.F., et al. 2000,J. Geophys. Res., 105, 7491
Xie H., et al. 2004, J. Geophys. Res., 109, A03109
Yashiro, S., et al. 2004, J. Geophys. Res., 109, A07106
Zhang et al., 2003,ApJ, 582, 520

G. Michale, Astronomical Obsrvatory of Jagiellonian University, Orla 171, Krakow, Poland. (michalek@oa.uj.edu.pl)

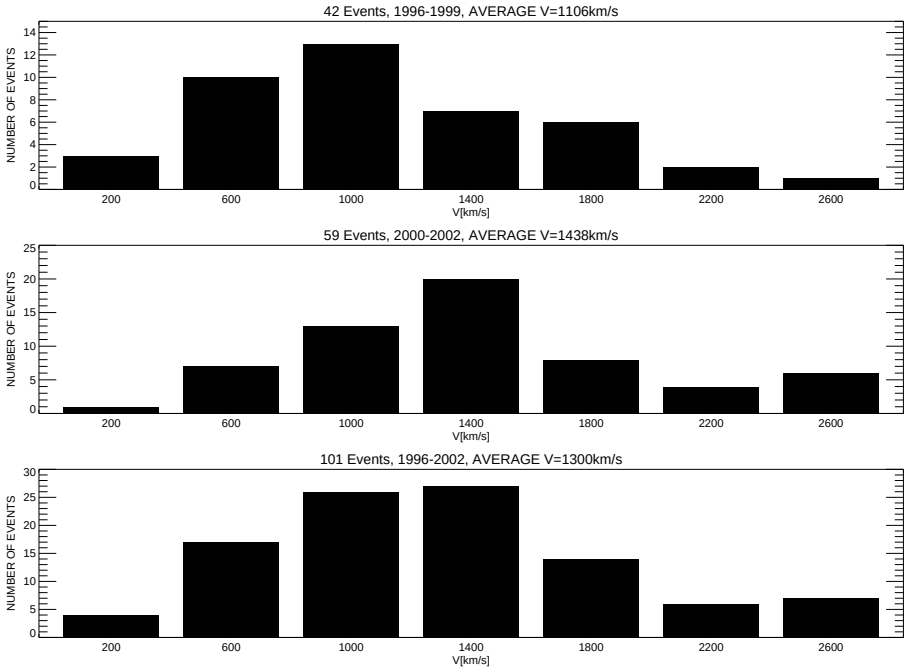

Figure 1. The histograms showing the distribution of space velocities (V) of HCMEs during the ascending (1996-1999) and maximum phases of solar activity (2000-2002) and for the whole considered period (1996-2002). From the histograms, it is evident that velocities of HCMEs increase significantly following the solar activity cycle.

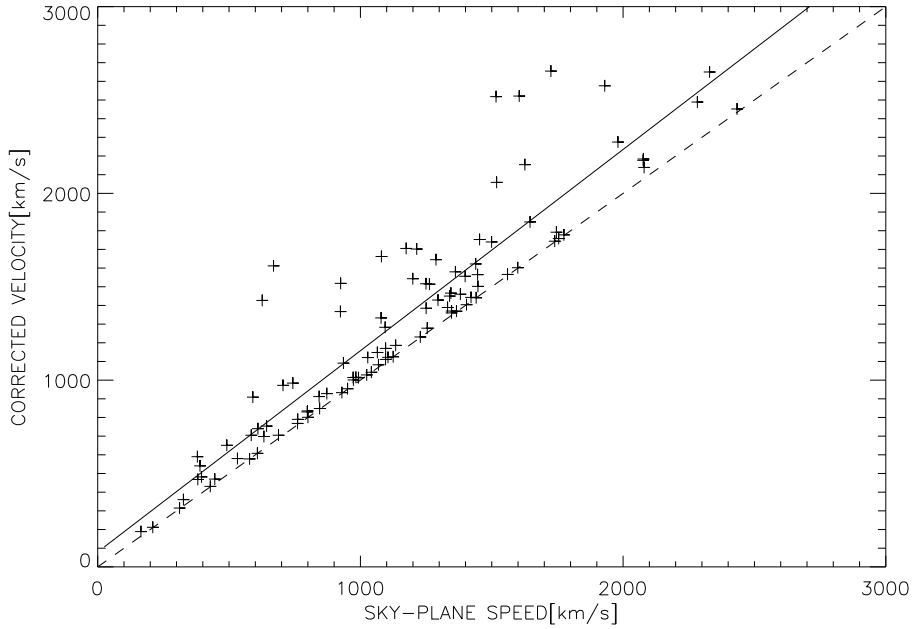

Figure 2. The plane of sky speed versus the corrected (space) speed of HCMEs. The solid line shows the linear fit to data points. The inclination of the linear fit demonstrates that the projection effect increases slightly with the speed of CMEs.

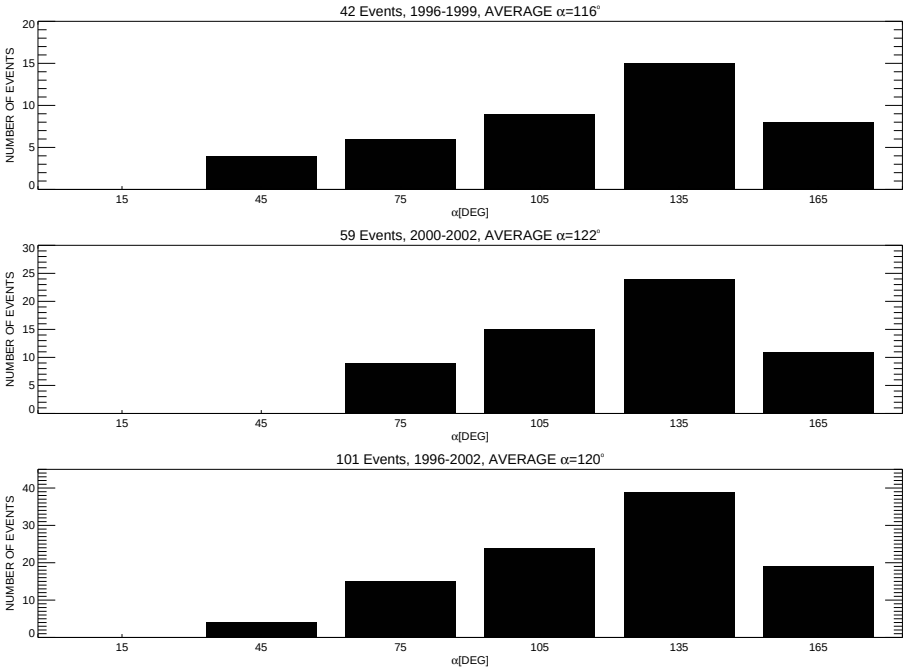

Figure 3. The histograms showing the distribution of width (α) of HCMEs during the ascending (1996-1999) and maximum phases of solar activity (2000-2002) and for the whole considered period (1996-2002). The average width of HCMEs does not change significantly with solar activity

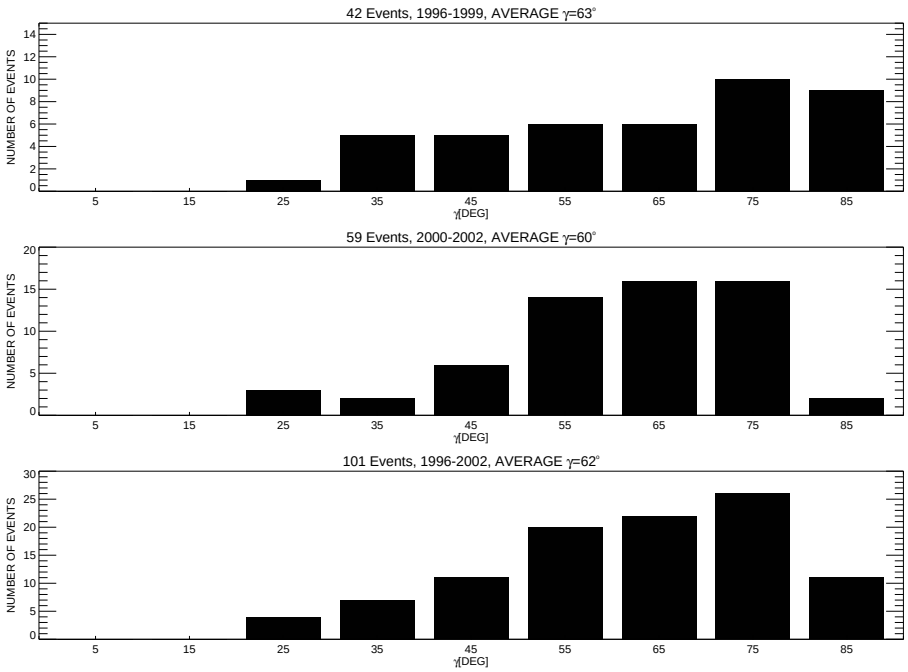

Figure 4. The histogram showing distribution of source location (γ) of HCMEs during the ascending (1996-1999) andmaximum phases of solar activity (2000-2002) and for the whole considered period (1996-2002). Histograms shows that the FHCMEs originate close to the Sun center with a maximum of distribution around $\gamma = 62^o$. The distribution of source location does not depend on the period of solar activity.

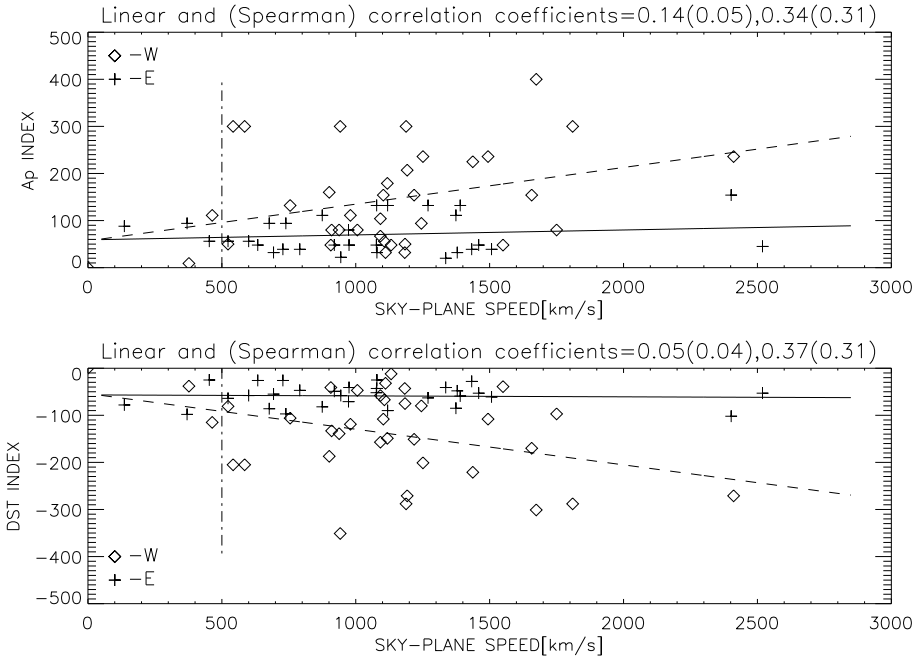

Figure 5. The scatter plots of the sky-plane speed versus Ap and D_{ST} indices. Diamond symbols represent events originating from the western hemisphere and cross symbols represent events originating from the eastern hemisphere. The solid lines are the linear fits to data points associated with eastern events, and the dashed lines are linear fits to data points associated with western events. The dot-dashed vertical lines indicate velocity limits above which HCMEs can cause severe ($D_{ST} \leq -150nT$) geomagnetic storms. Upon inspection of this figure, it is clear that the major geomagnetic storms can be generated by slow (speeds $\approx 500km/s$) and fast HCMEs originating in the western hemisphere.

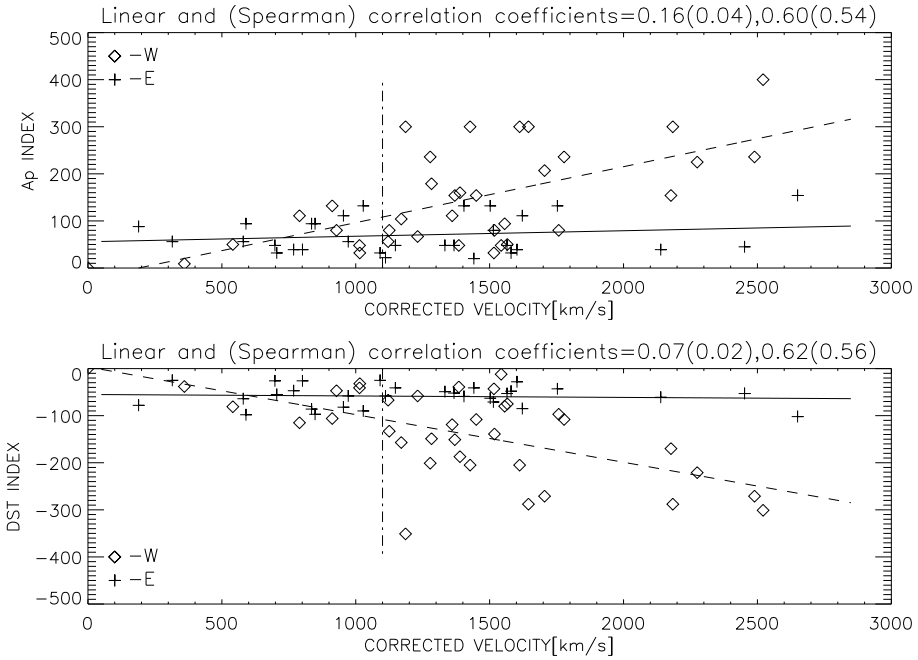

Figure 6. The scatter plots of the space velocity (V) versus Ap and D_{ST} indices. Diamond symbols represent events originating from the western hemisphere and cross symbols represent events originating from the eastern hemisphere. The solid lines are the linear fits to data points associated with, eastern events and the dashed lines are linear fits to data points associated with western events. The dot-dashed verticals lines indicate velocity limits above which HCMEs can cause significant geomagnetic storms ($D_{ST} \leq -150nT$). Upon inspection of this figure, it is clear that only very fast events ($V \geq 1100km/s$) originating in the western hemisphere can cause severe geomagnetic storms.

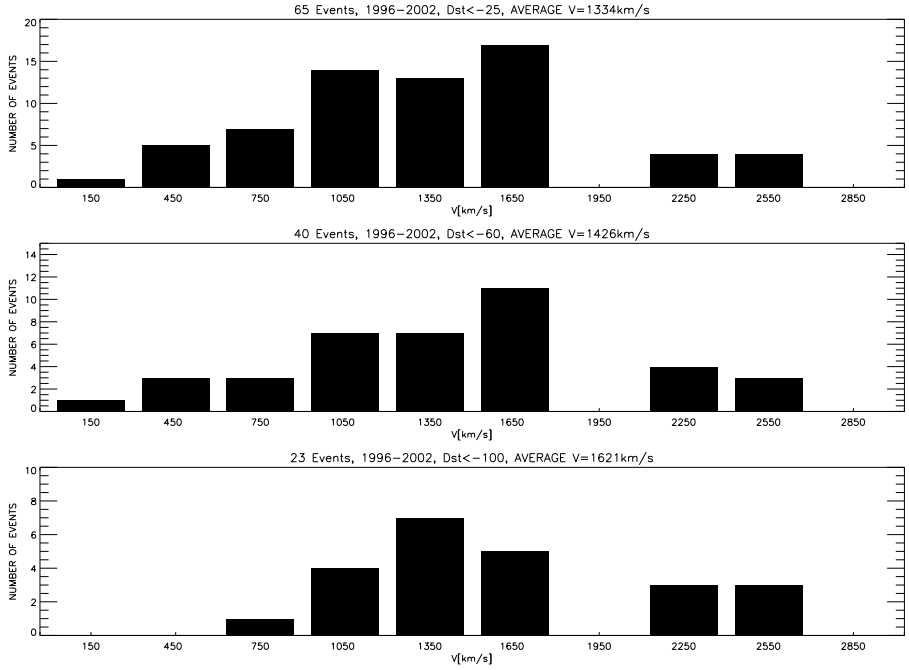

Figure 7. The histograms showing distribution of the space velocities (V) of FHCMEs which cause geomagnetic disturbance with D_{ST} index lower than $-25nT$, $-60nT$ and $-100nT$. These histograms demonstrate that geoeffectivenes of HCMEs depend on their space velocities and sever geomagnetic storms with $D_{ST} < -100nT$ can be caused by fast CMEs (with $V > 700km/s$) only.

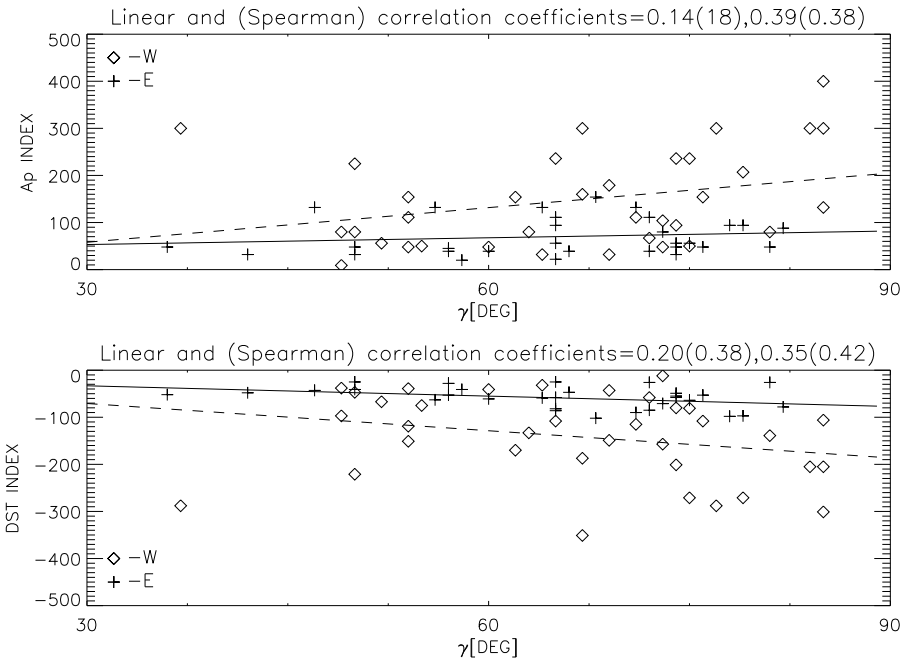

Figure 8. The scatter plots of the source location (γ) versus Ap and D_{ST} indices. Diamond symbols represent events originating from the western hemisphere and cross symbols represent events originating from the eastern hemisphere. The solid lines are the linear fits to the data points associated with eastern events, and the dashed lines are linear fits to data points associated with western events. It is clear that the western events originating close to the disk center ($\gamma \geq 65^o$) are more likely to cause the biggest geomagnetic storms.

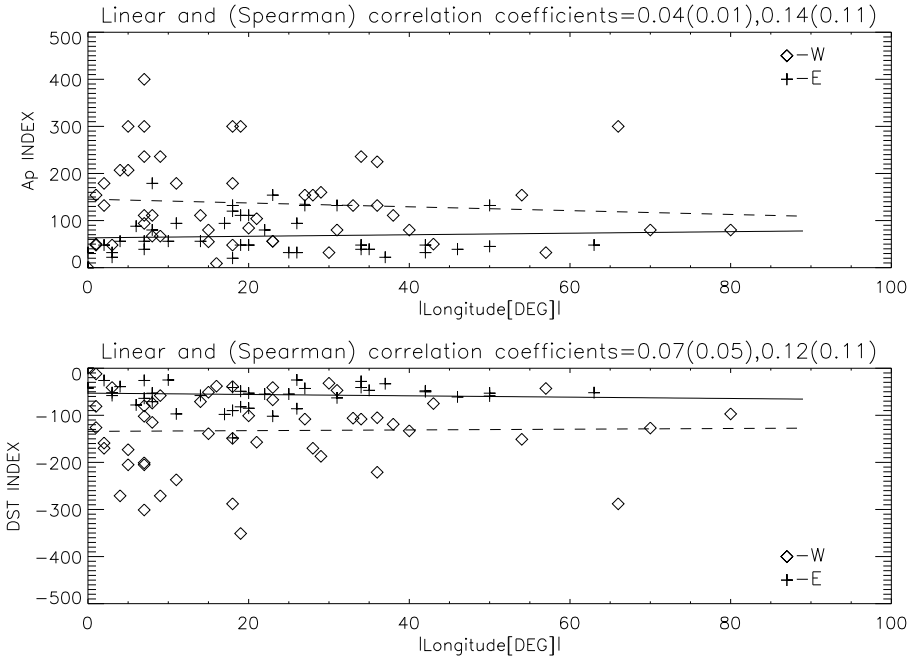

Figure 9. The scatter plots of absolute values of longitudes of H-alpha flares associated to HCMEs versus Ap and D_{ST} indices. Diamond symbols represent events originating from the western hemisphere and cross symbols represent events originating from the eastern hemisphere. The solid lines are the linear fits to the data points associated with eastern events, and the dashed lines are linear fits to data points associated with western events. Upon inspection of the figures, it is clear that the western events originating close to the disk center are more likely to cause the biggest geomagnetic storms.

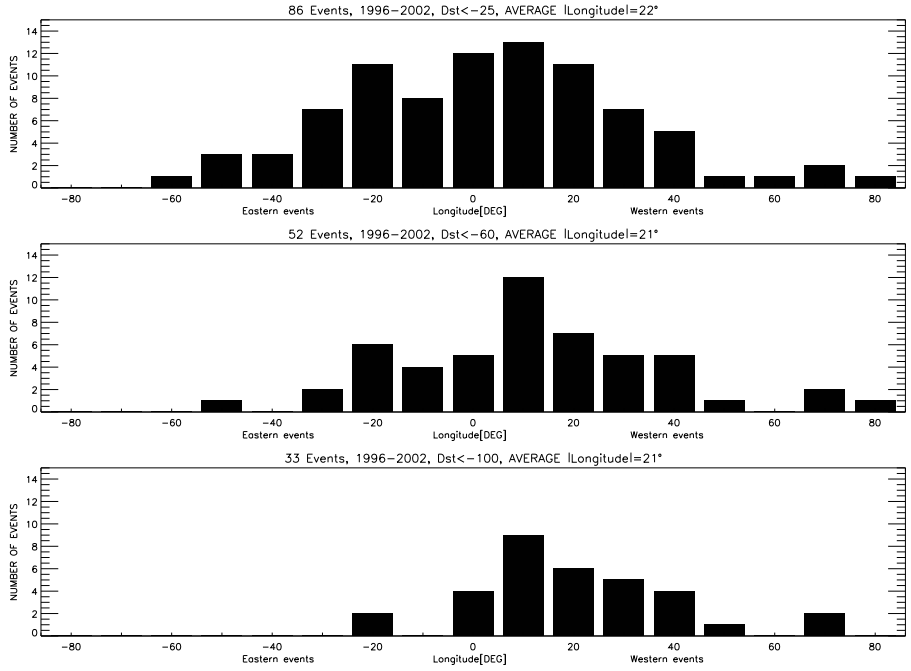

Figure 10. The histograms showing distribution of the longitude of HCMEs which cause geomagnetic disturbance with D_{ST} index lower than $-25nT$, $-60nT$ and $-100nT$. Upon inspection of the histograms, it is clear that the goeffectiveness of CMEs depends on the longitude of source location and that the severe geomagnetic disturbance ($D_{ST} < -100nT$) are mostly caused by the western events originating close to the disk center.

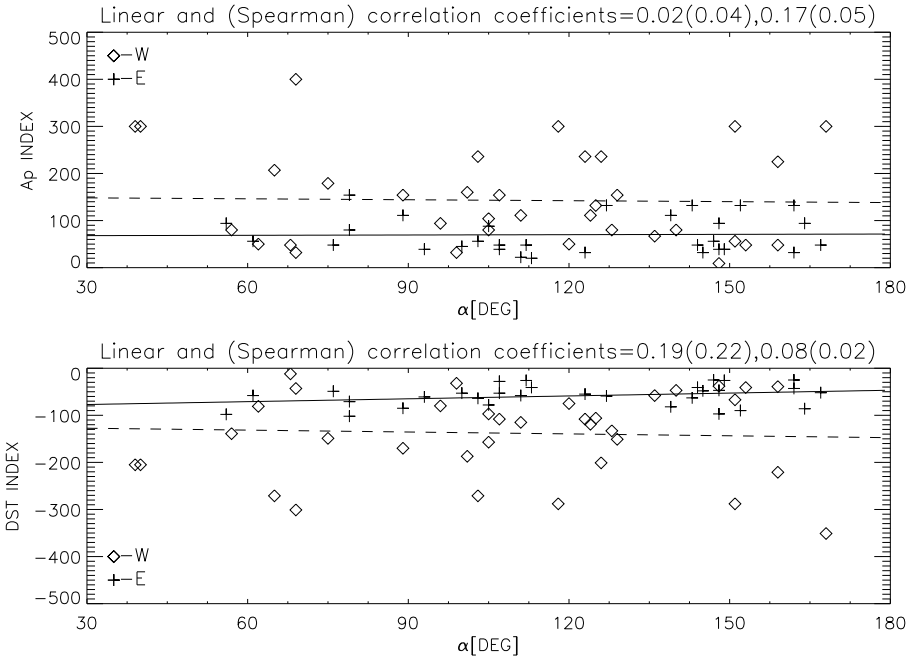

Figure 11. The scatter plots of the α versus Ap and D_{ST} indices. Diamond symbols represent events originating in the western hemisphere and cross symbols represent events originating in the eastern hemisphere. The solid lines are the linear fits to data points associated with eastern events, and the dashed lines are linear fits to data points associated with western events. The geoeffectiveness of CMEs depends

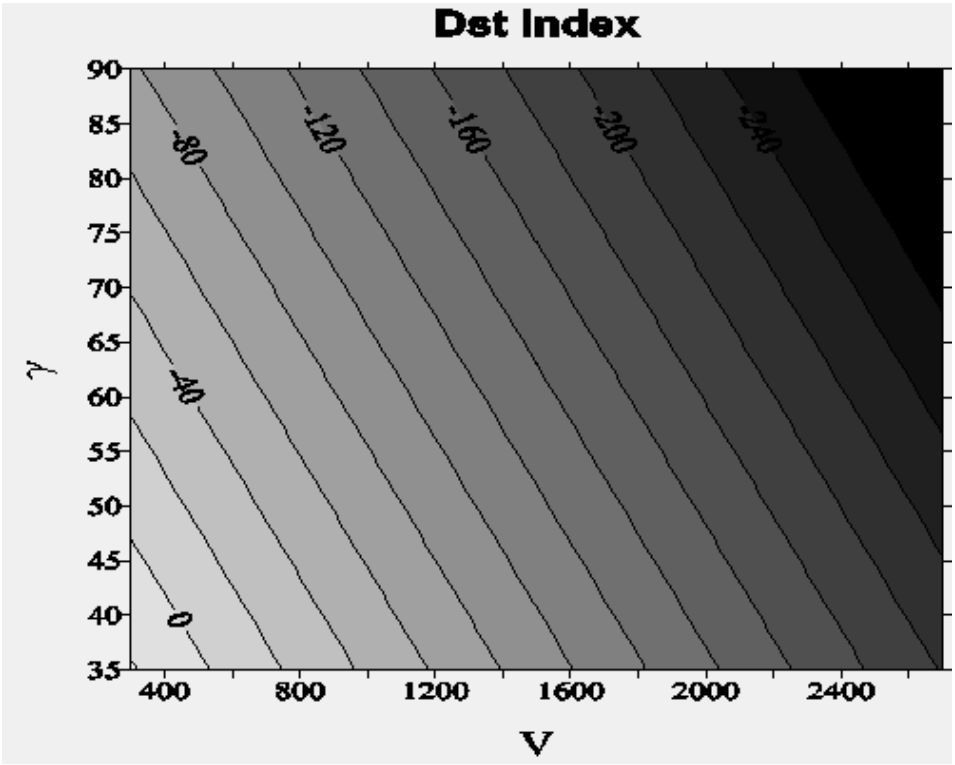

Figure 12. The contour map presenting D_{ST} index versus the space velocity (V) and the source location (γ). From the inspection of the picture we see that the strongest geomagnetic storms can occur for fast events originating close to the disk center.

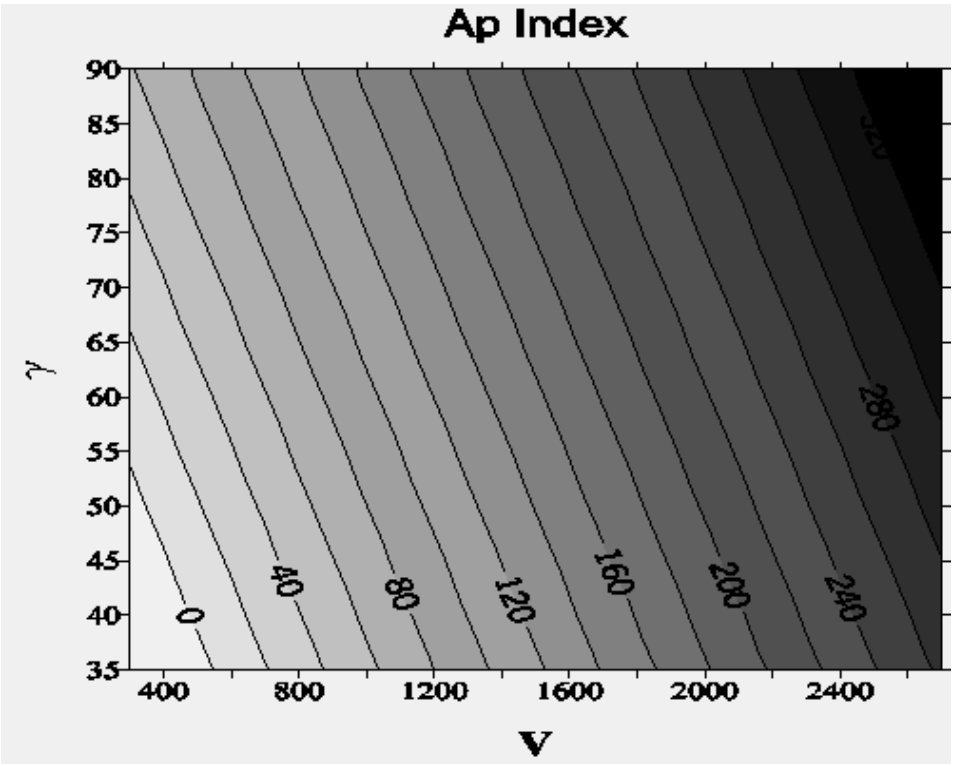

Figure 13. The contour map presenting Ap index versus the space velocity (V) and the source location (γ). From the inspection of the picture we see that the strongest geomagnetic storms can occur for fast events originating close to the disk center.

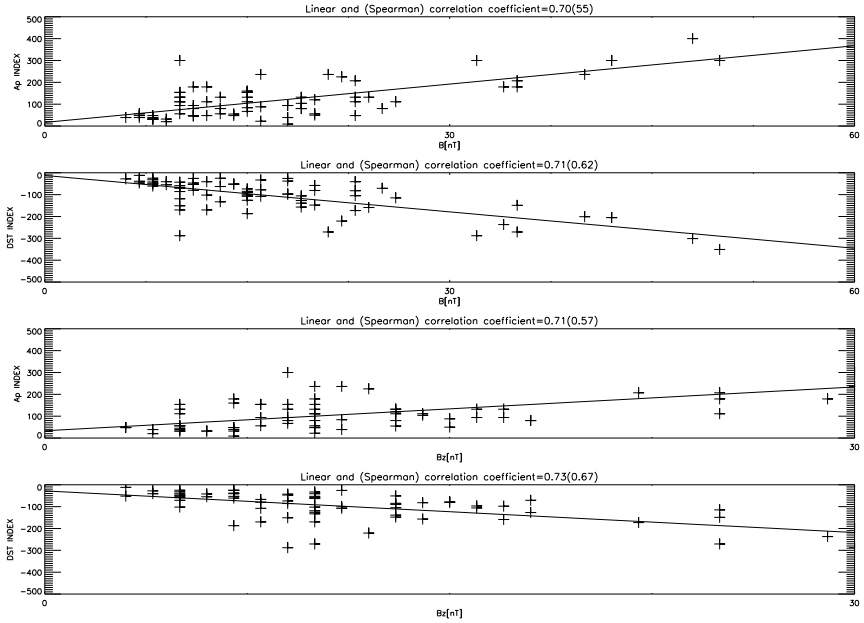

Figure 14. The scatter plots of the B and B_Z versus Ap and D_{ST} indices. Correlation between these parameters and geomagnetic indices is significant (correlation coefficient are > 0.50) and linear and (Spearman) coefficients are approximately equal 0.70(0.60) for (B) and (B_Z) as well.

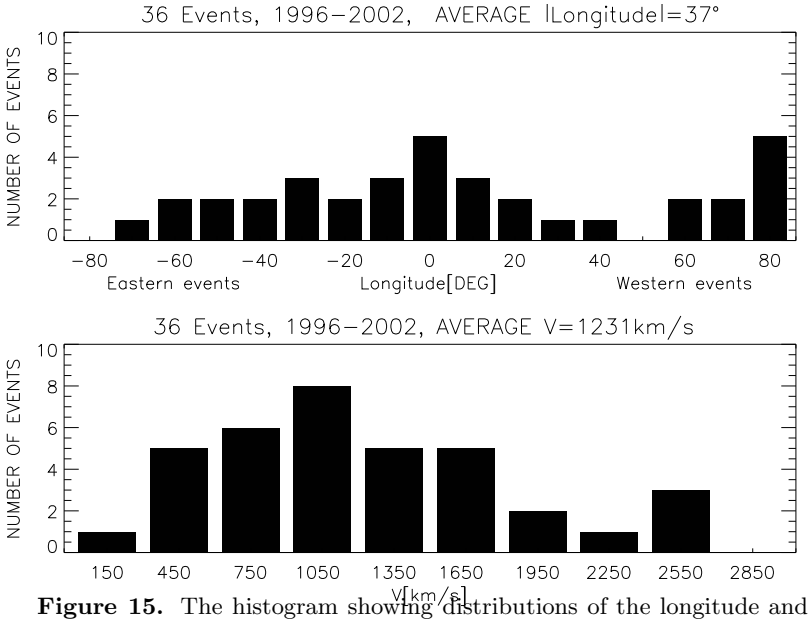

Figure 15. The histogram showing distributions of the longitude and space speed of non-geoeffective FHCMEs. The histograms show that these events originate from the whole solar disk and have velocities from $100km/s$ up to $2500km/s$.

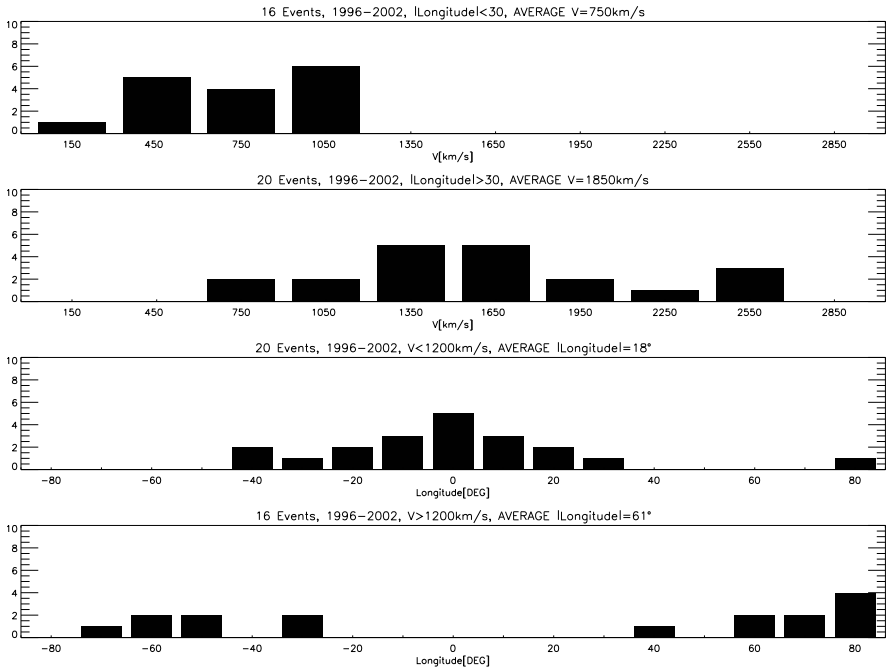

Figure 16. The histograms showing: space velocities for non-geoeffective FHCMEs originating close to the disk center ($|longitude| < 30^o$), space velocities for non-geoeffective FHCMEs originating close to the limb ($|longitude| > 30^o$), longitude for slow non-geoeffective FHCMEs ($V < 1200km/s$) and longitude for fast non-geoeffective FHCME ($V > 1200km/s$). Upon the inspection of the histograms (the first and last panel in the figure) it is clear that all fast HCMEs ($V > 1200km/s$) originating close to the disk center ($|longitud| < 30^0$) must be geoeffective.

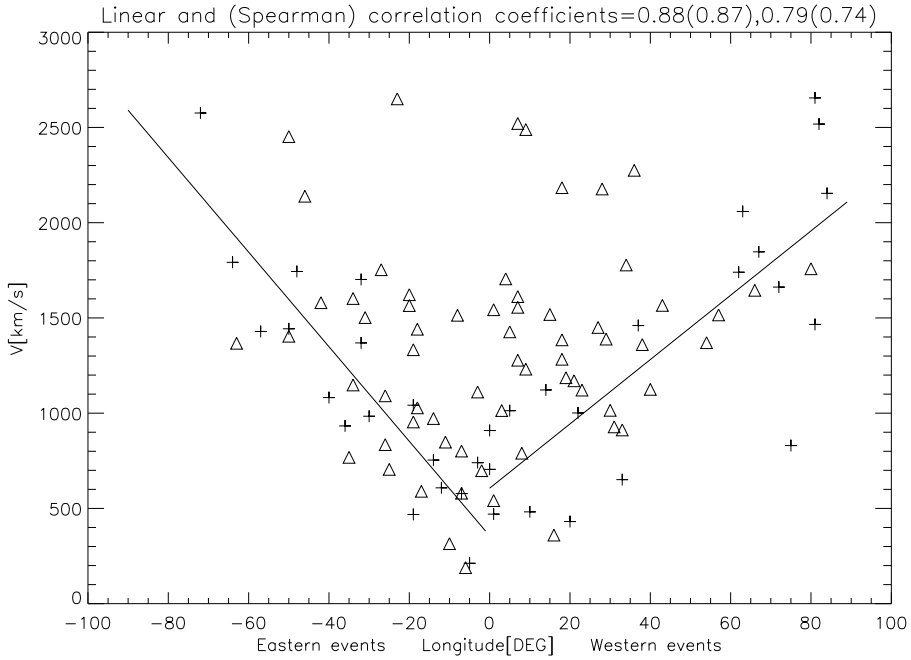

Figure 17. Figure shows the scatter plot of the space velocities versus longitude for all FHCMEs. Diamond symbols represent goeeffective and cross symbols non-geoeffective FHCMEs. The solid lines are linear fits for non-geoeffective events originating from the east and west hemisphere.Upon inspection of the figure, it is clear that geoeffective events are faster than the non-geoeffective events originating at the same longitude.

Table 1. The Table shows the list of frontside halo CMEs (1996-2002). The first four columns are from the SOHO/LASCO catalog and give date, time of first appearance in the coronagraph field of view, projected speed and position angle of the fastest part of the HCME. Parameters r, γ, α, and V, estimated from the cone model (Michalek et al. 2003), are shown in columns (5), (6), (7), and (8), respectively. In column (9) the source locations of the associated H-flares are presented. The changes of geomagnetic indices D_{ST} and Ap caused by the ICMEs are shown in columns 10 and 11. The last two columns (12 and 13) give the maximum value of magnitude (B) and southward component (B_Z) of magnetic field in the ICME.

List of halo CMEs

DATA	TIME	SPEED	PA	r	γ	α	V	Location	Dst	Ap	B	B_z
		km/ s	Deg	$\frac{1}{R_\odot}$	Deg	Deg	km/s				nT	nT
1996/12/02	15:35:05	538	270	0.77	39	110	830	S05W75	—	—	—	—
1997/01/06	15:10:42	136	182	0.13	82	105	189	S18E06	-78	88	16	-15
1997/04/07	14:27:44	875	126	0.42	65	139	954	S30E19	-82	111	23	-14
1997/05/12	06:30:09	464	277	0.32	71	111	790	N21W08	-115	111	26	-25
1997/08/30	01:30:35	370	65	0.21	78	56	590	N30E17	-98	94	18	-17
1997/09/17	20:28:48	377	274	0.65	49	148	360	N45W16	-38	09	18	-07
1997/09/28	01:08:33	359	66	0.53	57	131	212	N22E05	—	—	—	—
1997/10/21	18:03:45	523	30	0.24	75	103	580	N16E07	-64	56	—	—
1997/11/04	06:10:05	755	265	0.12	85	125	912	S14W33	-106	132	19	-16
1997/11/06	12:10:41	1556	261	0.82	34	153	2059	S18W63	—	—	—	—
1998/01/21	06:37:25	361	176	0.71	44	159	468	S57E19	—	—	—	—
1998/01/25	15:26:34	693	36	0.27	74	123	705	N21E25	-55	32	09	-06
1998/04/23	05:27:07	1618	113	0.61	59	126	1744	E15E48	—	—	—	—
1998/04/27	08:56:06	1385	79	0.35	69	118	1443	S16E50	—	—	—	—
1998/04/29	16:58:54	1374	16	0.30	72	89	1622	S17E20	-85	111	15	-13
1998/05/01	23:40:09	585	142	0.10	84	40	1427	S18W05	-205	300	42	-35
1998/05/02	05:31:56	542	143	0.10	85	39	1612	S20W07	-205	300	42	-35
1998/05/02	14:06:12	938	311	0.15	81	57	1518	S15W15	-139	80	19	-13
1998/11/04	07:54:07	523	0	0.25	75	62	541	N17W01	-81	50	20	-15
1998/11/05	02:02:52	380	264	0.18	79	88	482	N19W10	—	—	—	—
1998/11/05	20:44:02	1118	305	0.35	69	75	1283	N22W18	-149	179	35	-25
1998/11/24	02:30:05	1744	224	0.88	27	153	2655	S30W81	—	—	—	—
1998/11/27	08:30:05	434	—	—	—	—	—	S24E09	—	—	—	—
1998/12/18	18:09:50	1749	40	0.68	47	120	1792	N19E64	—	—	—	—
1999/05/03	06:06:05	1584	50	0.61	51	110	1369	N15E32	—	—	—	—
1999/05/10	05:50:05	920	80	0.27	74	76	1333	N16E19	-49	48	—	—
1999/06/12	21:26:08	465	—	—	—	—	—	N27W43	—	—	—	—
1999/06/22	18:54:05	1133	—	—	—	—	—	N22E37	-33	22	16	-10
1999/06/23	07:31:24	1006	—	—	—	—	—	N24E45	—	—	—	—
1999/06/24	13:31:24	975	314	0.63	50	144	1148	N24E34	-41	48	12	-07
1999/06/26	07:31:25	558	0	0.11	83	67	909	N25E00	—	—	—	—
1999/06/28	21:30:08	1083	—	—	—	—	—	N26W51	—	—	—	—
1999/06/29	07:31:26	634	10	0.15	81	112	698	N19E02	-26	48	11	-07
1999/06/29	18:54:07	438	—	—	—	—	—	S14E01	—	—	—	—
1999/06/30	11:54:07	406	23	0.16	80	92	705	S15E00	—	—	—	—
1999/07/25	13:31:21	1389	306	0.76	40	127	1466	N38W81	—	—	—	—
1999/07/28	05:30:05	457	—	—	—	—	—	S15E08	-53	179	11	-07
1999/07/28	09:06:05	456	—	—	—	—	—	S15E04	-39	56	07	-05
1999/09/20	06:06:05	604	—	—	—	—	—	S20W05	-173	207	23	-22
1999/10/14	09:26:05	1250	63	0.82	34	157	1702	N11E32	—	—	—	—
1999/12/22	02:30:05	570	14	0.75	40	162	984	N10E30	—	—	—	—
1999/12/22	19:31:22	605	24	0.65	69	141	1042	N24E19	—	—	—	—
2000/01/18	17:54:05	739	162	0.18	79	148	848	S19E11	-97	94	18	-16
2000/01/28	20:12:41	1177	—	—	—	—	—	S31W28	—	—	—	—
2000/02/08	09:30:05	1079	55	0.63	50	162	1091	N25E26	-25	32	08	-07
2000/02/09	19:54:17	910	218	0.44	63	128	1125	S17W40	-133	80	13	-10
2000/02/10	02:30:05	944	331	0.41	65	111	1111	N30E03	-58	22	—	—
2000/02/12	04:31:20	1107	335	0.61	52	151	1121	N26W23	-67	56	10	-08
2000/02/17	20:06:05	728	196	0.29	72	149	801	S29E07	-26	39	18	-11
2000/04/04	16:32:37	1188	304	0.79	37	151	1645	N16W66	-288	300	32	-30
2000/04/10	00:30:05	409	212	0.14	81	125	470	S14W01	—	—	—	—
2000/05/05	15:50:05	1594	269	0.85	32	146	2154	S16W84	—	—	—	—
2000/06/06	15:54:05	1119	6	0.32	71	152	1028	N20E18	-90	132	15	-13
2000/06/07	16:30:05	842	—	—	—	—	—	N23E03	-52	32	—	—
2000/06/10	17:08:05	1108	306	0.68	50	138	1460	N22W37	—	—	—	—
2000/07/07	10:26:05	453	198	0.42	65	147	315	N17E10	-25	56	13	-05
2000/07/11	13:27:23	1078	51	0.68	47	162	1753	N18E27	-43	132	10	-09
2000/07/14	10:54:07	1674	270	0.10	85	69	2521	N22W07	-301	400	48	-40
2000/07/25	03:30:05	528	—	—	—	—	—	N06W08	-74	67	15	-09
2000/08/09	16:30:05	702	—	—	—	—	—	N11W11	-237	179	34	-29
2000/09/12	11:54:05	1550	216	0.58	54	159	1385	S17W18	-39	48	—	—
2000/09/15	21:50:07	257	—	—	—	—	—	N13E03	—	—	—	—
2000/09/16	05:18:14	1251	21	0.27	74	126	1278	N14W07	-201	236	40	-30
2000/09/25	02:50:05	587	—	—	—	—	—	S11W59	—	—	—	—
2000/10/02	03:50:05	525	144	0.41	65	131	578	S09E07	—	—	—	—
2000/10/02	20:26:05	569	—	—	—	—	—	S10W02	-170	179	12	-10

Table 2. List of halo CMEs

DATA	TIME	SPEED	PA	r	γ	α	V	Location	Dst	Ap	B	B_z
		km/ s	Deg	$\frac{1}{R_\odot}$	Deg	Deg	km/s				nT	nT
2000/10/09	23:50:05	798	—	—	—	—	—	N01W14	-71	111	10	-05
2000/10/24	08:26:05	800	—	—	—	—	—	S20E70	—	—	—	—
2000/10/25	08:26:05	770	—	—	—	—	—	N17W70	-127	80	19	-18
2000/11/01	16:26:08	801	—	—	—	—	—	S20E42	-50	48	—	—
2000/11/03	18:26:06	291	—	—	—	—	—	N02W02	-159	132	24	-17
2000/11/23	06:06:05	492	230	0.72	43	168	651	S22W33	—	—	—	—
2000/11/24	05:30:05	994	352	0.45	62	147	1013	N20W05	—	—	—	—
2000/11/24	15:30:05	1245	324	0.26	74	96	1556	N22W07	-80	94	11	-08
2000/11/24	22:06:05	1005	312	0.56	55	130	1122	N21W14	—	—	—	—
2000/11/25	01:31:58	2519	75	0.54	57	100	2452	N07E50	-53	45	11	-05
2000/11/25	09:30:17	675	—	—	—	—	—	N18W24	—	—	—	—
2000/11/25	19:31:57	671	—	—	—	—	—	N20W23	—	—	—	—
2000/11/26	17:06:05	980	283	0.58	54	124	1360	N18W38	-119	111	10	-10
2000/12/18	11:50:05	510	15	0.05	87	105	740	N14E03	—	—	—	—
2001/01/10	00:54:05	832	102	0.55	56	122	933	N13E36	—	—	10	-05
2001/01/20	19:31:50	839	109	0.51	58	134	1082	S07E40	—	—	—	—
2001/01/20	21:30:08	1507	78	0.49	60	93	2139	S07E46	-61	39	08	-07
2001/02/11	01:31:48	1183	294	0.64	69	69	1516	N24W57	-43	32	—	—
2001/02/15	13:54:05	625	18	0.39	66	134	608	N07E12	—	—	07	-06
2001/03/19	05:26:05	389	—	—	—	—	—	S05W00	-42	32	08	-06
2001/03/24	20:50:05	906	—	—	—	—	—	N15E22	-55	80	—	—
2001/03/25	17:06:05	677	19	0.42	65	164	835	N16E26	-86	94	10	-09
2001/03/29	10:26:05	942	277	0.38	67	168	1186	N20W19	-351	300	50	-45
2001/04/05	17:06:05	1390	83	0.43	64	127	1404	S24E50	-59	132	10	-05
2001/04/06	19:30:02	1270	124	0.54	56	143	1502	S21E31	-63	132	13	-10
2001/04/09	15:54:02	1192	213	0.18	79	65	1705	S21W04	-271	207	35	-25
2001/04/10	05:30:00	2411	187	0.25	75	103	2489	S23W09	-271	236	21	-10
2001/04/11	13:31:48	1103	229	0.23	76	107	1450	S22W27	-108	154	15	-08
2001/04/12	10:31:29	1184	251	0.57	55	120	1566	S19W43	-75	50	—	—
2001/04/26	12:30:05	1006	46	0.64	50	140	928	N17W31	-47	80	11	-09
2001/08/14	16:01:28	618	—	—	—	—	—	N16W36	-105	132	23	-13
2001/08/25	16:50:05	1433	127	0.54	57	107	1602	S17E34	-28	39	06	-04
2001/08/31	16:11:33	310	—	—	—	—	—	N19E33	—	—	—	—
2001/09/11	14:54:05	791	74	0.39	66	148	768	N13E35	-47	39	07	-05
2001/09/24	10:30:59	2402	147	0.36	68	79	2650	S12E23	-102	154	15	-05
2001/09/28	08:54:34	846	—	—	—	—	—	N10E18	-148	120	20	-13
2001/10/09	11:30:05	973	174	0.27	73	79	1514	S28E08	-71	80	25	-18
2001/10/19	16:50:05	901	268	0.37	67	101	1389	N15W29	-187	160	15	-07
2001/10/22	15:06:05	1336	121	0.51	58	113	1441	S21E18	-41	20	09	-04
2001/10/25	15:26:05	1092	203	0.27	73	105	1170	S16W21	-157	104	19	-14
2001/11/01	22:30:05	453	—	—	—	—	—	N12W23	-41	56	—	—
2001/11/03	19:20:05	457	307	0.25	75	138	431	N04W20	—	—	—	—
2001/11/04	16:35:06	1810	246	0.21	77	118	2184	N06W18	-288	300	10	-09
2001/11/17	05:30:06	1379	65	0.73	42	145	1580	S13E42	-48	32	08	-05
2001/11/21	14:06:05	518	—	—	—	—	—	S13W18	—	—	—	—
2001/11/22	20:30:33	1443	221	0.74	42	138	1847	S25W67	—	—	—	—
2001/11/22	23:30:05	1437	68	0.74	42	159	2275	S17W36	-221	225	22	-12
2001/11/28	17:30:06	500	—	—	—	—	—	N14E16	—	—	07	-03
2001/12/13	14:54:06	864	—	—	—	—	—	N16E09	—	—	—	—
2002/01/04	09:30:05	896	—	—	—	—	—	N38E87	—	—	—	—
2002/01/08	17:54:05	1794	—	—	—	—	—	S18E79	-51	48	—	—
2002/02/20	06:30:05	952	270	0.88	27	153	1662	N12W72	—	—	—	—
2002/03/14	17:06:06	907	140	0.75	41	132	1429	S23E57	—	—	—	—
2002/03/15	23:06:06	907	276	0.49	60	153	1014	S08W03	-41	48	23	-10
2002/03/18	02:54:06	989	257	0.31	71	115	1001	S15W22	—	—	08	-05
2002/03/20	17:30:05	308	—	—	—	—	—	S17W20	-101	84	15	-11
2002/03/22	11:06:05	1750	261	0.64	49	105	1758	S20W80	-97	80	—	—
2002/04/15	03:50:05	720	—	—	—	—	—	S15W01	-126	154	15	-10
2002/04/17	08:26:05	1218	283	0.58	54	129	1370	S16W54	-151	154	10	-09
2 2002/05/07	04:06:05	720	120	0.32	70	77	754	S22E14	—	—	08	-03
2002/05/08	13:50:05	614	—	—	—	—	—	S12W07	-102	111	12	-10
2002/05/16	00:50:05	600	140	0.26	74	61	972	S22E14	-58	56	20	-10
2002/05/22	03:50:05	1494	247	0.45	65	123	1778	S30W34	-108	236	16	-11
2002/05/28	16:26:05	1244	224	0.89	26	158	2518	N06W82	—	—	—	—
2002/07/15	20:30:05	1132	3	0.28	73	68	1543	N19W01	-12	48	07	-03
2002/07/18	08:06:08	1111	279	0.43	64	99	1015	N19W30	-32	32	08	-05
2002/07/23	01:31:51	1726	87	0.87	29	141	2576	S13E72	—	—	—	—
2002/07/26	22:06:10	818	—	—	—	—	—	S19E26	—	—	—	—
2002/07/29	12:07:33	556	—	—	—	—	—	N10W15	-51	55	14	-13
2002/08/16	12:30:05	1459	121	0.23	76	107	1565	S14E20	-53	48	14	-10
2002/08/22	02:06:06	1005	233	0.77	39	139	1740	S05W62	—	—	—	—
2002/08/24	01:27:19	1878	—	—	—	—	—	S02E81	-45	39	—	—
2002/09/05	16:54:06	1657	115	0.46	62	89	2177	N04W28	-170	154	10	-08
2002/11/09	13:31:45	1838	—	—	—	—	—	S12W29	—	—	—	—
2002/11/10	03:30:11	1516	—	—	—	—	—	S12W37	—	—	—	—
2002/11/24	20:30:05	1077	48	0.79	36	167	1367	N15E63	-52	48	08	-03
2002/12/08	23:54:05	1339	—	—	—	—	—	S18E70	—	—	—	—

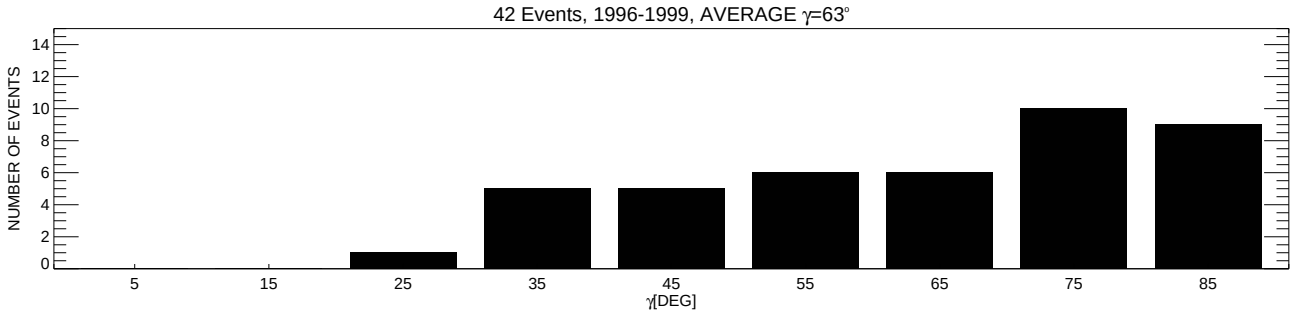
42 Events, 1996-1999, AVERAGE γ=63°
NUMBER OF EVENTS
0
2
4
6
8
10
12
14
5
15
25
35
45
55
65
75
85
γ[DEG]

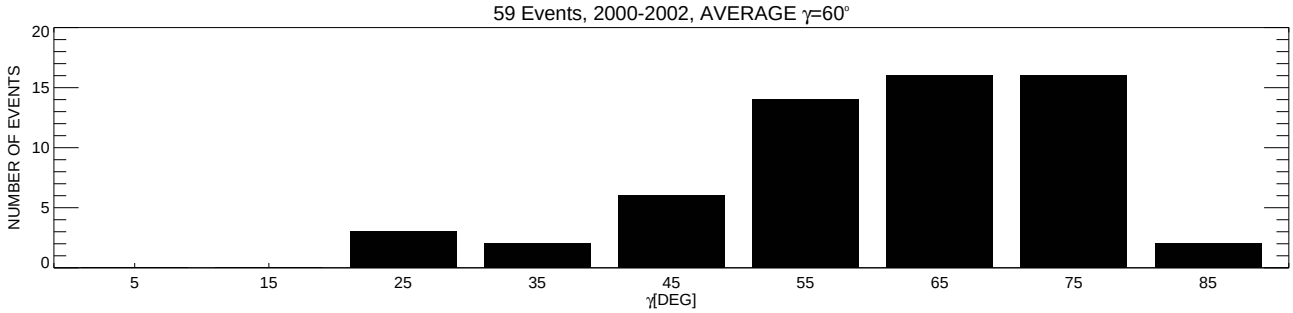
59 Events, 2000-2002, AVERAGE γ=60°
NUMBER OF EVENTS
0
5
10
15
20
5
15
25
35
45
55
65
75
85
γ[DEG]

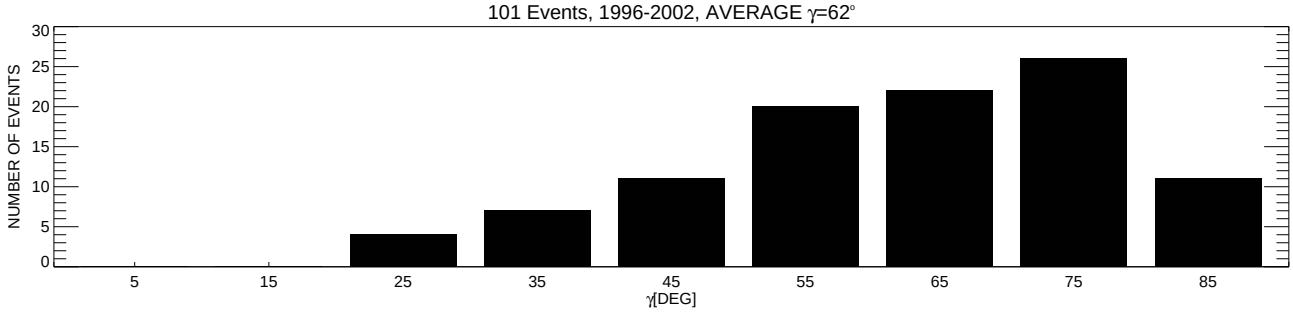
101 Events, 1996-2002, AVERAGE γ=62°
NUMBER OF EVENTS
0
5
10
15
20
25
30
5
15
25
35
45
55
65
75
85
γ[DEG]